Polyhedron 55 (2013) 45–48

Contents lists available at SciVerse ScienceDirect

Polyhedron

journal homepage: www.elsevier.com/locate/poly

Formation of polyphosphorus ligands mediated by zirconium and hafnium complexes

Aleksandra Wiśniewska [a], Agnieszka Łapczuk-Krygier [b], Katarzyna Baranowska [a], Jarosław Chojnacki [a], Eberhard Matern [c], Jerzy Pikies [a], Rafał Grubba [a,*]

[a] Chemical Faculty, Department of Inorganic Chemistry, Gdansk University of Technology, G. Narutowicza St. 11/12, Pl-80-233 Gdansk, Poland
[b] Institute of Organic Chemistry and Technology, Cracow University of Technology, Warszawska 24, 31-155 Cracow, Poland
[c] Institut für Anorganische Chemie, Universität Karlsruhe (TH), D-76128 Karlsruhe, Engesserstr. 15, Germany

ARTICLE INFO

Article history:
Received 17 October 2012
Accepted 12 February 2013
Available online 28 February 2013

Keywords:
P ligands
Polyphosphorus compounds
Zirconium
Hafnium

ABSTRACT

The reactions of R_2P–$P(SiMe_3)Li$ (R = ^{t}Bu, ^{i}Pr, ^{i}Pr$_2$N) with $[Cp_2MCl_2]$ (M = Zr, Hf), $[Cp^*CpZrCl_2]$ and $[CpZrCl_3]$ yielded polyphosphorus (mainly hexaphosphorus) compounds which can be viewed as intermediates between R_2P–$P(SiMe_3)Li$ and derivatives of 1,2,3,4-tetraphosphabicyclo[1.1.0] butane. Thus R_2P–$P(SiMe_3)Li$ can act as a building block for the formation of the P_2 ligand and the R_2P–$P(P_2)$ and R_2P–$P(P_2)P$–PR_2 moieties. Solid state structures of zirconium(IV) and hafnium(IV) complexes with R_2P–$P(P_2)$ and R_2P–$P(P_2)P$–PR_2 ligands were established by X-ray studies.

1. Introduction

The reactivity of lithium derivatives of diphosphanes, R_2P–$P(SiMe_3)Li$ (R = ^{t}Bu, ^{i}Pr, Et$_2$N and ^{i}Pr$_2$N), towards transition metal complexes, $[L_nMCl_2]$, has been the subject of our studies. Generally this precursor in donor solvents can lead to phosphanylphosphinidene (R_2P–P) complexes. In the case of M = Zr and Cp (η^5-C_5H_5) as a spectator ligand, these reactions lead to a terminal complex with the ^{t}Bu$_2$P–P group or to dinuclear complexes with this group in the side-on and terminal alignment [1]. The use of $(Et_2N)_2P$–$P(SiMe_3)Li$ leads to the formation of the dimeric complex $[Cp_2Zr\{\mu\text{-}P\text{–}P(NEt_2)_2\}_2ZrCp_2]$ with $(Et_2N)_2P$–P ligands in the bridging mode [2]. The introduction of spectator imido ligands results in the formation of anionic tungsten(VI) complexes with a $R_2P{=}P$ moiety in a side-on geometry [3]. Similarly the reactions of $[L_2PtCl_2]$ (L = tertiary phosphane) with R_2P–$P(SiMe_3)Li$ yield Pt(0) complexes with a side-on bonded $R_2P{=}P$ moiety [4]. The reactions of these precursors depend very much on the sterical influence of the spectator ligands. With small spectator ligands, such as Cp and Cp^{Me} (Cp^{Me} = C_5H_4Me), these reactions give rise to phosphanylphosphido (R_2P–$PSiMe_3$) ligands [1–3,5,6]. If the spectator ligands are of medium size (indenyl), the formed phosphanylphosphido complexes are overcrowded and probably undergo a cleavage of the P–P bond in the ligand [7]. Stephan et al. demonstrated a similar behaviour of phosphinidene complexes. An overcrowding at the Zr center may induce P–C bond cleavage in a PR ligand and therefore provide access to substituent free P-complexes of Zr [8].

Now we present the results of our studies on the reactivity of R_2P–$P(SiMe_3)Li$ (R = ^{t}Bu, ^{i}Pr and ^{i}Pr$_2$N) towards $[Cp_2ZrCl_2]$, $[CpZrCl_3]$, $[CpCp^*ZrCl_2]$ and $[Cp_2HfCl_2]$ under conditions which lead to polyphosphorus compounds. Some types (but not all) of our polyphosphorus skeletons are obtainable *via* activation of white phosphorus P_4 mediated by early transition metal complexes, for reviews see [9–11]. Thus the reactions involving R_2P–$P(SiMe_3)Li$ precursors can occur the usual way *via* P_4 functionalization.

2. Experimental

Toluene and THF were dried over Na/benzophenone and distilled under nitrogen. Pentane was dried over Na/benzophenone/diglyme and distilled under nitrogen. All manipulations were performed in flame-dried Schlenk type glassware on a vacuum line. Literature methods were used to prepare R_2P–$P(SiMe_3)Li{\cdot}nL$ (R = ^{t}Bu, ^{i}Pr, N^{i}Pr$_2$; L = THF, DME) [12]. ^{31}P NMR and ^{1}H spectra were recorded on Bruker AC250, Bruker AMX300 and Bruker Av400 MHz spectrometers (external standard 85% H_3PO_4) at ambient temperature. Simulation of the spectra was performed with the aid of BRUKER software [13]. Experimental diffraction data were collected on a KM4CCD kappa-geometry diffractometer, equipped with a Sapphire2 CCD detector. An enhanced X-ray Mo Kα radiation source with a graphite monochromator was used. Determina-

* Corresponding author. Tel.: +48 58 347 1714.
E-mail address: grubba@pg.gda.pl (R. Grubba).

0277-5387/$ - see front matter © 2013 Elsevier Ltd. All rights reserved.
http://dx.doi.org/10.1016/j.poly.2013.02.046

tion of the unit cells and data collection were carried out at 150 or 120 K. Data reduction, absorption correction, space group determination, solution and refinement were made using the CRYSALISPRO software package [14]. The structure of **5** was processed by the SQUEEZE/PLATON program [15] to remove electron density of the disordered solvent (*ca.* 74 e^-), equivalent to two molecules of THF (volume: 239 Å^3).

2.1. Reaction of $^tBu_2P$–P(SiMe$_3$)Li with [Cp_2ZrCl_2] and an excess of $PhPMe_2$

A solution of 0.411 g (1.028 mmol) $^tBu_2P$–P(SiMe$_3$)Li·2THF in 2 mL DME was added dropwise to a solution of 0.156 g (0.726 mmol) [Cp_2ZrCl_2] and 0.7 mL $PhPMe_2$ in 2 mL DME at −40 °C over 30 min. The solution immediately turned deep red. The solution was left for 6 h at ambient temperature and turned initially brown and then green. The solvent was evaporated almost completely under reduced pressure and the residue was extracted with pentane (2 mL). The extract was filtered; the volume was reduced to 1 mL under reduced pressure and stored at room temperature. After 1 week, deep blue–black crystals of [Cp_2(PMe_2Ph)Zr(η^1-P–P$^tBu_2$)] were formed and separated. The mother liquor turned blue. After 1 month at 4 °C, a small amount of yellow–green crystals of [{Zr($PPhMe_2$)-Cp_2}{*cyclo*-P_3(P^tBu_2)}] (**2**) separated (0.030 g). In the mother liquor we established the formation of **1**.

1 $^{31}P\{^1H\}$ NMR (mother liquor), ppm: P4 183.9, P2 70.3, P1 16.5, P5 5.92, P3 −150.4. J_{P1-P4} 13.1 Hz, J_{P4-P5} 27.9 Hz, J_{P3-P4} 383.2 Hz, J_{P1-P2} 254.3 Hz, J_{P2-P3} 99.2 Hz, J_{P1-P3} 329.5 Hz, J_{P3-P5} 7.6 Hz.

2 $^{31}P\{^1H\}$ NMR (crystals dissolved in C_6D_6, for labelling of P atoms see Fig. 1), ppm: P1 −181.9, P2 −200.7, P3 −138.4, P4 75.2, P5 11.6. $^1J_{P1-P2}$ 300.7 Hz, $^1J_{P1-P3}$ 201.3 Hz, $^2J_{P1-P4}$ 52.9 Hz, $^2J_{P1-P5}$ 10.7 Hz, $^1J_{P2-P3}$ 185.3 Hz, $^2J_{P2-P4}$ 64.8 Hz, $^2J_{P2-P5}$ 43.1 Hz, $^1J_{P3-P4}$ 255.6 Hz, $^3J_{P3-P5}$ 19.3 Hz, $^4J_{P4-P5}$ 4.6 Hz.

2.2. Reaction of $^iPr_2P$–P(SiMe$_3$)Li with [Cp_2HfCl_2] in THF

A solution of 0.121 g (0.828 mmol) [Cp_2HfCl_2] in 5 mL THF was added dropwise to a solution of 0.457 g (0.828 mmol) $^iPr_2P$–P(SiMe$_3$)Li·2.6THF in 2 mL THF at −40 °C. The resulting solution turned orange. The solution was left at ambient temperature overnight and turned deep red. The volatile compounds and the solvent were evaporated under reduced pressure and the residue was extracted with 5 mL toluene. The extract was examined by $^{31}P\{^1H\}$, ^{31}P and ^1H NMR. The solution was then reduced to ≈1.5 mL and stored at −30 °C. After 6 days deep red crystals of **3** formed (0.028 g).

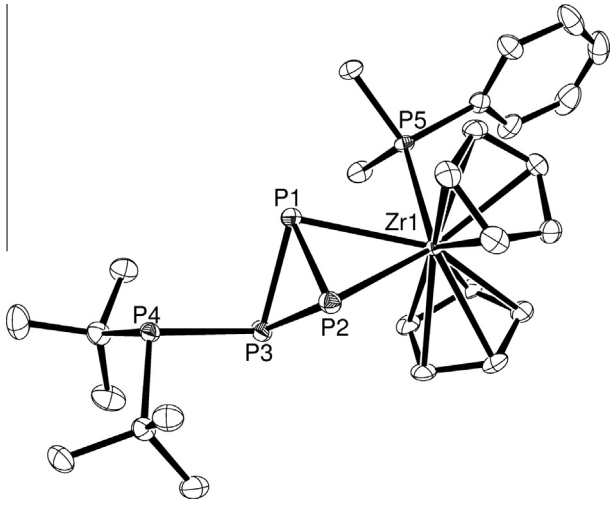

Fig. 1. Molecular structure of **2** showing the atom-numbering scheme (50% probability displacement ellipsoids), important bond lengths (Å) and bond angles (°). H atoms have been omitted. Zr1–P1 2.7337(4), Zr1–P2 2.6862(7), Zr1–P5 2.7561(7), P1–P2 2.1596(10), P1–P3 2.2177(9), P2–P3 2.2026(10), P3–P4 2.2390(9), P1–Zr–P2 46.96(4), P1–P3–P4 98.43(4), P2–P3–P4 100.09(4), P1–P3–P2 58.49(3), C11–P4–P3 102.70(9), C15–P4–P3 99.24(9), C11–P4–C15 109.60(12), C11–P4–P3 102.70(9), P3–P1–P2–Zr1 108.47(3).

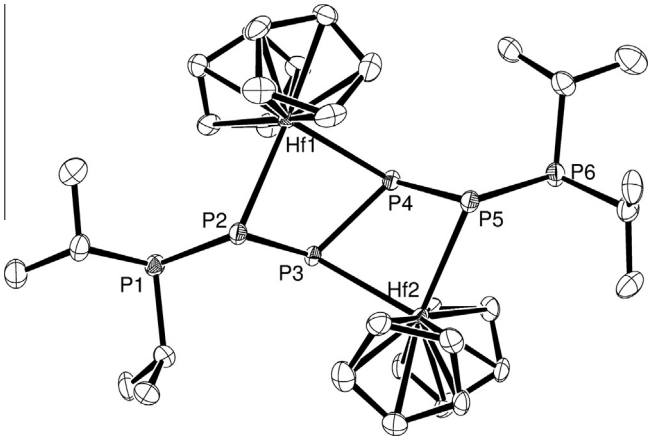

Fig. 2. Molecular structure of **3** showing the atom-numbering scheme (50% probability displacement ellipsoids), important bond lengths (Å) and bond angles (°). H atoms have been omitted. Hf1–P2 2.631(2), Hf1–P3(no bond) 2.971(2) Hf1–P4 2.621(2), P1–P2 2.211(3), P2–P3 2.240(3), P3–P4 2.262(3), P2–Hf1–P4 89.23(7), P2–P3–Hf2 114.3(1), P4–P3–Hf2 57.85(8), P3–P4–P5 108.4(1), Hf2–P5–P6 113.4(1), P4–P5–P6 98.79(1).

3 $^{31}P\{^1H\}$ NMR (from mother liquor, for labelling of P atoms see Fig. 2), ppm: AA′MM′XX″ P1, P6 42.4; P2, P5 19.4; P3, P4 −70.0; $^1J_{P1-P2}$ −225.5 Hz, $^2J_{P1-P3}$ 127.5 Hz, $^3J_{P1-P4}$ 9.7 Hz, $^4J_{P1-P5}$ 5.9 Hz, $^5J_{P1-P6}$ 3.3 Hz, $^1J_{P2-P3}$ −265.2 Hz, $^2J_{P2-P4}$ −2.5 Hz, $^3J_{P2-P5}$ −3.5 Hz, $^4J_{P2-P6}$ 5.9 Hz, $^1J_{P3-P4}$ −341.9 Hz.

Additionally two unknown compounds, **3a** and **3b**, and several known compounds were found.

3a $^{31}P\{^1H\}$ NMR, ppm: P1 35.7, P2 −29.8, $^1J_{P1-P2}$ −422.6 Hz. **3b** $^{31}P\{^1H\}$ NMR, ppm: P1 31.1, P2 −114.7, $^1J_{P1-P2}$ −410.5 Hz. Known compounds: $^iPr_2P$–P(SiMe$_3$)$_2$, $^iPr_2P$–P(SiMe$_3$)H, $^iPr_2P$–PH–P^iPr_2, $^iPr_2PH$.

2.3. Reaction of $^tBu_2P$–P(SiMe$_3$)Li with [$Cp^*CpZrCl_2$] in THF

A solution of 0.186 g (0.492 mmol) [$Cp^*CpZrCl_2$] in 5 mL THF was added dropwise to a solution of 0.361 g (0.972 mmol) $^tBu_2P$–P(SiMe$_3$)Li·2THF in 3 mL THF at −70 °C over 1 h. The solution immediately turned deep red. The solution was left overnight at ambient temperature. The solvent was then evaporated under reduced pressure to dryness and the residue was extracted with pentane (5 mL). The extract was filtered; the volume was reduced to ≈2 mL under reduced pressure and stored at −70 °C. After 1 month, a small amount of red crystals of **4** precipitated (0.040 g).

4 $^{31}P\{^1H\}$ NMR (mother liquor, see Fig. 3 for labelling), ppm: P1 73.33, P2 53.78, P3 −201.83, P4 −97.12, P5 68.70, P6 79.32, J_{P1-P2} 10.45 Hz, J_{P1-P3} −306.80 Hz, J_{P1-P4} 121.92 Hz, J_{P1-P5} −232.90 Hz, J_{P1-P6} 1.96 Hz, J_{P2-P3} −264.01 Hz, J_{P2-P4} −188.35 Hz, J_{P2-P5} 5.75 Hz, J_{P2-P6} 47.98 Hz, J_{P3-P4} −158.94 Hz, J_{P3-P5} 126.61 Hz, J_{P3-P6} 133.60 Hz, J_{P4-P5} −4.55 Hz, J_{P4-P6} −232.60 Hz, J_{P5-P6} 0.05 Hz.

2.4. Reaction of ($^iPr_2N$)$_2$P–P(SiMe$_3$)Li with [$Cp^*CpZrCl_2$] in THF

A solution of 0.187 g (0.508 mmol) [$Cp^*CpZrCl_2$] in 4 mL THF was added dropwise to a solution of 0.521 g (0.998 mmol) ($^iPr_2N$)$_2$-P–P(SiMe$_3$)Li·2.5·THF in 3 mL THF at −70 °C over 1 h. The solution immediately turned orange. The solution was left for 2 days at

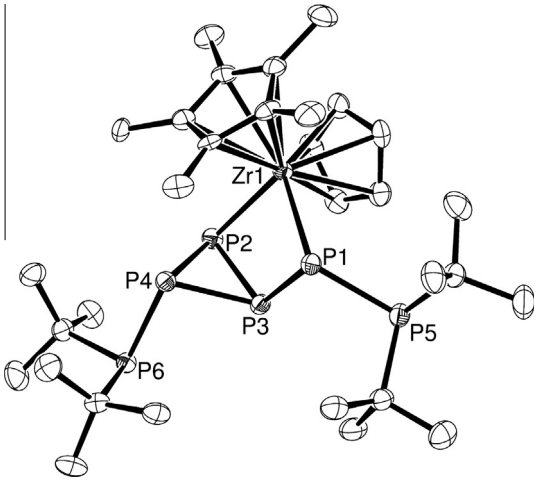

Fig. 3. Molecular structure of **4** showing the atom-numbering scheme (50% probability displacement ellipsoids), important bond lengths (Å) and bond angles (°). H atoms have been omitted. Zr1–P1 2.642(1), Zr1–P2 2.622(2), P1–P3 2.231(2), P1–P5 2.237(2), P2–P3 2.226(2), P2–P4 2.195(2), P3–P4 2.205(2), P4–P6 2.231(2), P1–Zr1–P2 90.37(5), P3–P1–Zr1 76.20(6), P3–P1–P5 96.41(8), P5–P1–Zr1 120.01(7), P3–P2–Zr1 76.71(6), P4–P2–Zr1 95.73(7), P3–P2–P4 59.85(7), P1–P3–P2 113.83(9), P1–P3–P4 101.86(8), P2–P4–P3 60.77(7), P2–P4–P6 104.78(8), P3–P4–P6 97.10(8).

ambient temperature and it turned brown. The solvent was then evaporated under reduced pressure to dryness and the residue was extracted with pentane (5 mL). The extract was filtered; the volume was reduced to ≈2 mL under reduced pressure and stored at 4 °C. After 3 weeks a small amount of red crystals of **5** precipitated (0.020 g).

3. Results and discussion

The main reactions of $R_2P–P(SiMe_3)Li$ (R = ^{t}Bu, ^{i}Pr and ^{i}Pr$_2$N) towards $[Cp_2ZrCl_2]$ and $[Cp_2HfCl_2]$ leading to phosphanylphosphinidene [1] and phosphanylphosphido complexes [1,2] are relatively well understood. However, these reactions are accompanied by some side processes:

^{t}Bu$_2$P–P(SiMe$_3$)Li reacts with $[Cp_2ZrCl_2]$ and an excess of $PhPMe_2$ yielding mainly the known terminal phosphanylphosphinidene complex $[Cp_2(PhPMe_2)Zr(\eta^1\text{-}P–P^tBu_2)]$. In some runs we observed, by ^{31}P NMR, the formation of two additional pentaphosphorus complexes **1** and **2** (Scheme 1) after 2 weeks in the reaction solution. So far we have not been able to isolate **1**. In solution it displays a $^{31}P\{^1H\}$ NMR first order spectrum (ppm): P4 183.9, P2 70.3, P1 16.5, P5 5.92, P3 −150.4, $J_{P1–P4}$ 13.1 Hz, $J_{P4–P5}$ 27.9 Hz, $J_{P3–P4}$ 383.2 Hz, $J_{P1–P2}$ 254.3 Hz, $J_{P2–P3}$ 99.2 Hz, $J_{P1–P3}$ 329.5 Hz, $J_{P3–P5}$ 7.6 Hz. An examination of the P–P coupling pattern suggests that a ^{t}Bu$_2$P4–P3 bond and a P3–P1–P2 triangle are placed around the $ZrCp_2$(P5PhMe$_2$) centre, but that only P4 and P3 couple with P5PhMe$_2$ (Scheme 1). Thus a skeleton similar to that of **2** is probable.

Compound **2** was isolated from the mother liquor (pentane solution) after isolation of $[Cp_2(PhPMe_2)Zr(\eta^1\text{-}P–P^tBu_2)]$, and was characterized by XRD (Fig. 1) and its ^{31}P NMR spectrum.

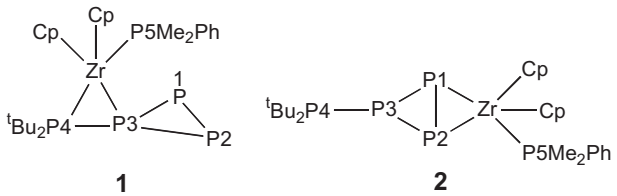

Scheme 1.

The X-ray structural investigation of **2** (triclinic, $P\bar{1}$ group, $Z = 2$) indicates a relatively short P1–P2 bond (2.1596 Å), which can be explained as a double P–P bond coordinated side-on to the Zr center. The P3–P1 (2.2173 Å) and P3–P2 (2.2026 Å) bond lengths are in the range for P–P single bonds. P3–P4 (2.2390 Å) is slightly longer. The geometry around the Zr1 atom is typical for a bent $[Cp_2ZrL_3]$ system [16], which forces Zr and the ligand atoms P1, P2 and P5 to lie in a common plane. The angle between the planes P1–P2–P3 and P1–P2–Zr1 is 108.47°. The spatial alignment of these two planes and the P–P distances in the P1–P2–P3–P4 fragment closely resemble that of 2,4-bis[bis(diisopropylamino)phosphanyl]-1,2,3,4-tetraphosphabicyclo[1.1.0]butane, with a similarly short P1–P2 distance of 2.1610 Å [17]. According to isolobal relationships [18], the metal fragment $ZrCp_2(PhPMe_2)$, (d^2ML_7) can be regarded as replacing a phosphinidene fragment. Thus **2** can be treated as an isolobal analogue of an 1,2,3,4-tetraphosphabicyclo[1.1.0] butane derivative. The ^{31}P NMR data of **2** (first order spin system) clearly support the similarity of these two skeletons. For **2**:, the P2, P3 and P4 peaks are at −200.7, −138.4 and 75.2 ppm, respectively, whilst for $(^tBu_2P–P)_2(\mu\text{-}P_2)$ (AA′MM′X$_2$ spin system) the related values are −318.5, −141.4 and 65.0 ppm [19].

The mechanism for the formation of the P1–P4 part in the skeleton of **2** is not known. Generally two ways seem to be possible. The first way may proceed *via* a formation of a P_2 zirconium complex as a result of a P–P bond cleavage in the ^{t}Bu$_2$P–P ligand (similar to the P–C bond cleavage in the zirconium phosphinidene complexes [8]) followed by a ^{t}Bu$_2$P–P transfer. This assumption is supported by the existence of a bridged complex, $[(Cp^*_2Zr)_2(\mu\text{-}P_2)]$ [20], and by the ability of ^{t}Bu$_2$P–P(SiMe$_3$)Li to form a bridging P_2 ligand [21].

The second way may formally be an insertion reaction of two P atoms into a Zr–P bond in the terminal complex $[Cp_2(PhPMe_2)Zr(\eta^1\text{-}P–P^tBu_2)]$. The source of these P atoms is not known, but lithiated silyl derivatives of diphosphanes in polar solvents undergo sequences of redistribution reactions forming phosphorus rich compounds together with $P(SiMe_3)_3$ and $(Me_3Si)_2PLi$ [22]. To the best of our knowledge, the P skeleton of **2** is not accessible *via* reactions of transition metal complexes with P_4 [9–11].

The reaction of ^{i}Pr$_2$P–P(SiMe$_3$)Li with $[Cp_2HfCl_2]$ in THF yields several known compounds (^{i}Pr$_2$P–P(SiMe$_3$)$_2$, ^{i}Pr$_2$P–P(SiMe$_3$)H, ^{i}Pr$_2$P–PH–P^{i}Pr$_2$ and ^{i}Pr$_2$PH) and two unknown compounds **3a** (2 P atoms) and **3b** (2 P atoms), together with **3** (see Section 2). Crystallization of the reaction products from toluene solution yielded red crystals of **3** (Fig. 2).

Compound **3** can formally be seen as the product of an insertion of two $[Cp_2Hf]$ groups into the P–P bonds of the 2,4-bis[diisopropylphosphanyl]-1,2,3,4-tetraphosphabicyclo[1.1.0]butane skeleton. **3** (monoclinic, $P2_1/n$ group, $Z = 4$) displays a distorted tetrahedral geometry around the Hf atoms with a P2–Hf1–P4 angle of 89.23°, typical for $[Cp_2HfL_2]$ compounds [23]. All the P–P bond lengths indicate their single bond character. All P atoms display a pyramidal geometry, the sum of angles around the P atoms is 302.11, 281.69 and 299.50° for P1, P2 and P3, respectively.

^{31}P NMR data of **3** in solution (AA'MM'XX' spin system) support the XRD results. The coupling constants $^1J_{P1–P2}$ −225.5 Hz, $^1J_{P2–P3}$ −265.2 Hz and $^1J_{P3–P4}$ −341.9 Hz indicate the single bond character of the related bonds. Such a skeleton (with two early transition metal centres) was not observed in the reactions of early transition metal complexes with P_4 [9–11].

Reactions of $R_2P–P(SiMe_3)Li$ with $[Cp^*CpZrCl_2]$ do not lead to complexes with R_2PP or $R_2PP(SiMe_3)$ ligands, probably due to the sterically demanding Cp* groups. In the case of R = ^{t}Bu, the mononuclear P_6 compound **4** (Fig. 3) was isolated in moderate yield. The mother liquor additionally contained ^{t}Bu$_2$P–P(SiMe$_3$)$_2$, ^{t}Bu$_2$P–P(SiMe$_3$)H, ^{t}Bu$_2$P–PH–P^{t}Bu$_2$, ^{t}Bu$_2$PH and P(SiMe$_3$)$_3$. In the case of R = ^{i}Pr$_2$N, compound **5** (Fig. 4) was isolated, albeit in a low yield.

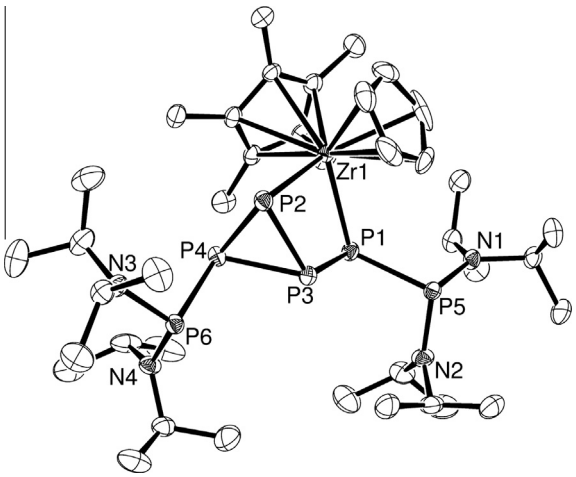

Fig. 4. Molecular structure of **5** showing the atom-numbering scheme (50% probability displacement ellipsoids), important bond lengths (Å) and bond angles (°). H atoms have been omitted. Zr1–P1 2.624(1), Zr1–P2 2.630(1), P1–P3 2.243(1), P1–P5 2.264(1), P2–P3 2.236(1), P2–P4 2.191(1), P3–P4 2.208(1), P4–P6 2.244(1), P1–Zr1–P2 90.93(2), P3–P1–Zr1 77.02(3), P3–P1–P5 92.77(3), P5–P1–Zr1 117.00(3), P3–P2–Zr1 77.01(3), P4–P2–Zr1 95.04(3), P3–P2–P4 59.82(3), P1–P3–P2 113.49(4), P1–P3–P4 104.25(4), P2–P4–P3 61.07(3), P2–P4–P6 102.73(4), P3–P4–P6 98.16(4), N1–P5–P1 98.49(8), N2–P5–P1 103.05(8), N1–P5–N2 108.9(1), N3–P6–P4 101.34(8), N4–P6–P4 97.74(8), N3–P6–N4 109.8 (1).

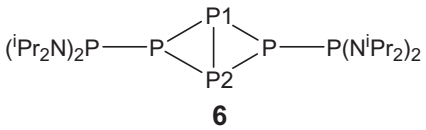

6

Scheme 2.

In the mother liquor we detected $(^{i}Pr_2N)_2P–P(SiMe_3)$, $(^{i}Pr_2N)_2P–P(SiMe_3)H$, $P(SiMe_3)_2H$, $(^{i}Pr_2N)_2P–P(N^{i}Pr_2)_2$ (strong singlet) and $P(SiMe_3)_3$, together with small amounts of unknown polyphosphorus compounds.

A similar compound (R = $SiMe_3$) was previously obtained in the reaction of $[Cp_2Zr\{P(SiMe_3)_2\}_2]$ with P_4 [24]. The labelling of the P atoms in **4** and **5** is the same as in [24].

Compounds **4** (monoclinic, $P2_1/c$ group, $Z = 4$), **5** (triclinic, $P\bar{1}$ group, $Z = 2$) and 1,1,6,6-tetrakis(trimethylsilyl)(P^2–P^4)-hexaphosphane-P^3,P^5-zirconocene [24] display very similar spatial alignments. Both compounds **4** and **5** indicate a distorted tetrahedral geometry around the Zr atoms with P1–Zr1–P2 angles of 90.37° (for **4**) and 90.93° (for **5**). All the P atoms exhibit a pyramidal geometry. The triangles P2,P3,P4 resemble the fragment of a P_4 molecule. ^{31}P NMR data of **4** (first order spectrum) indicate that this compound is identical in the solid state and in solution. Our results prove that this unusually stable P1–P6 skeleton is formed not only *via* splitting of a P–P bond in a P_4 molecule but also *via* reactions of molecules containing a P–PR_2 moiety as well.

$[CpZrCl_3]$ reacts with $(^{i}Pr_2N)_2P–P(SiMe_3)Li$ yielding a complex mixture of polyphosphorus compounds. In the ^{31}P NMR spectrum of the mother liquor we found the P1,P2 signal of **6** [17] (Scheme 2), together with the signals of $(^{i}Pr_2N)_2P–P(\mu_2\text{-}PN^{i}Pr_2)_2PSiMe_3$ [2], with strong signals of $(^{i}Pr_2N)_2P–P(SiMe_3)_2$, $(^{i}Pr_2N)_2P–P(SiMe_3)H$, $(^{i}Pr_2N)_2P–P(N^{i}Pr_2)_2$ and $(^{i}Pr_2N)_2PH$.

Similar compounds were formed in the thermal rearrangement of $^{t}Bu_2P–P = P(Me)\ ^{t}Bu_2$ [19] and in the reaction of P_4 with $(^{i}Pr_2N)\{(Me_3Si)_2N\}P–P\{N(SiMe_3)_2\}(N^{i}Pr_2)$ [25].

4. Conclusion

Our results prove that the formation of the 1,2,3,4-tetraphosphabicyclo[1.1.0] butane skeleton is probably thermodynamically very favorable. It is formed either from molecules which contain P–PR_2 groups, such as $^{t}Bu_2P–P = P(Me)\ ^{t}Bu_2$ [19] or $R_2P–P(SiMe_3)Li$, or maybe *via* P_4 functionalization as well. Thus the P–PR_2 group can act as a precursor for a P_2 ligand [22] as well as for the $R_2P–P(P_2)$ moiety (compound **2**), and for the $R_2P–P(P_2)P–PR_2$ moiety (compounds **3**, **4**, **5** and **6**). The formation of the 1,2,3,4-tetraphosphabicyclo[1.1.0]butane skeleton results from a P–P bond splitting in the P–PR_2 group. The side products (especially the formation of a large amount of $(^{i}Pr_2N)_2P–P(N^{i}Pr_2)_2$) support a radical mechanism of these cleavages.

Acknowledgements

J.P. and R.G. thank the Polish Ministry of Science and Higher Education (Grant No. N N204 271535) for financial support. A.Ł.-K. thanks the Polish Ministry of Science and Higher Education (Grant No. N N204 145038) for financial support.

Appendix A. Supplementary data

CCDC 905598-905601 contains the supplementary crystallographic data for **2**–**5**. These data can be obtained free of charge via http://www.ccdc.cam.ac.uk/conts/retrieving.html, or from the Cambridge Crystallographic Data Centre, 12 Union Road, Cambridge CB2 1EZ, UK; fax: (+44) 1223-336-033; or e-mail: deposit@ccdc.cam.ac.uk.

References

[1] J. Pikies, E. Baum, E. Matern, J. Chojnacki, R. Grubba, A. Robaszkiewicz, Chem. Commun. (2004) 2478.
[2] R. Grubba, A. Wiśniewska, K. Baranowska, E. Matern, J. Pikies, Dalton Trans. 40 (2011) 2017.
[3] R. Grubba, K. Baranowska, J. Chojnacki, J. Pikies, Eur. J. Inorg. Chem. 20 (2012) 3263.
[4] W. Domańska-Babul, J. Chojnacki, E. Matern, J. Pikies, Dalton Trans. (2009) 146.
[5] R. Grubba, A. Wiśniewska, K. Baranowska, E. Matern, J. Pikies, Polyhedron 30 (2011) 1238.
[6] a R. Grubba, K. Baranowska, D. Gudat, J. Pikies, Organometallics 30 (2011) 6655;
b T. Kruczyński, R. Grubba, K. Baranowska, J. Pikies, Polyhedron 39 (2012) 25.
[7] A. Łapczuk-Krygier, K. Baranowska, Ł. Ponikiewski, E. Matern, J. Pikies, Inorg. Chim. Acta 387 (2012) 361.
[8] M.C. Fermin, J. Ho, D.W. Stephan, Organometallics 14 (1995) 4247.
[9] M. Ehses, A. Romerosa, M. Peruzzini, Top. Curr. Chem. 220 (2002) 107.
[10] M. Peruzzini, L. Gonsalvi, A. Romerosa, Chem. Soc. Rev. 34 (2005) 1038.
[11] B.M. Cossairt, N.A. Piro, C.C. Cummins, Chem. Rev. 110 (2010) 4164.
[12] W. Domańska-Babul, K. Baranowska, R. Grubba, E. Matern, J. Pikies, Polyhedron 26 (2007) 5491.
[13] a Programs WINNMR and WINDAISY, Bruker Daltonik, Bremen, 1999.;
b G. Hägele, M. Engelhardt, W. Boenigk, Simulation und automatisierte Analyse von NMR-Spektren, VCH, Weinheim, 1987.
[14] Program CRYSALISPRO, Version 1.171, Oxford Diffraction, Abingdon, England, 2008.
[15] Program package PLATON including the SQUEEZE procedure A.L. Spek, J. Appl. Crystallogr. 36 (2003) 7.
[16] T.A. Albright, J.K. Burdett, M.-H. Whangbo, Orbital Interactions in Chemistry, John Wiley & Sons, 1984. p. 349.
[17] A. Łapczuk-Krygier, K. Baranowska, J. Pikies, Acta Crystallogr., Sect. E64 (2008) o2427.
[18] R. Hoffman, Angew. Chem. 94 (1982) 725.
[19] E. Matern, G. Fritz, J. Pikies, Z. Anorg. Allg. Chem. 623 (1997) 1769.
[20] M.C. Fermin, J. Ho, D.W. Stephan, J. Am. Chem. Soc. 116 (1994) 6033.
[21] W. Domańska-Babul, J. Chojnacki, E. Matern, J. Pikies, J. Organomet. Chem. 692 (2007) 3640.
[22] G. Fritz, K. Stoll, Z. Anorg. Allg. Chem. 538 (1986) 78.
[23] A. Wiśniewska, K. Baranowska, J. Pikies, Acta Crystallogr., Sect. E63 (2007) m2174.
[24] E. Hey, M.F. Lappert, J.L. Atwood, S.G. Bott, J. Chem. Soc., Chem. Commun. (1987) 597.
[25] J.P. Bezombes, P.B. Hitchcock, M.F. Lappert, J.E. Nycz, Dalton Trans. (2004) 499.